

SHC 2012

## Development of a 5 kW cooling capacity ammonia-water absorption chiller for solar cooling applications

François Boudéhenn <sup>a\*</sup>, Hélène Demasles <sup>a</sup>, Joël Wyttenbach <sup>a</sup>, Xavier Jobard <sup>a</sup>,  
David Chèze <sup>a</sup>, Philippe Papillon <sup>a</sup>

<sup>a</sup> CEA LITEN INES, 50 avenue du Lac Léman, 73377, Le Bourget du Lac, France

---

### Abstract

The development of a small capacity absorption chiller and the numerical and experimental results are presented in this paper. The prototype is a thermally driven ammonia-water absorption chiller of 5 kW cooling capacity for solar cooling applications. The chiller was developed in an industrial perspective with a goal of overall compactness and using commercially available components. In order to characterize various component technologies and different optimization components, the prototype is monitored with temperature, pressure and mass flow rate accurate sensors. The resulting chiller, characterized by a reduced load in ammonia-water solution and the use of brazed plate heat exchanger, has shown good performance during the preliminary tests. A comparison with the expected numerical results is given.

© 2012 Published by Elsevier Ltd. Selection and peer-review under responsibility of the PSE AG

*Keywords:* Heat driven ammonia-water absorption chiller; solar cooling; small cooling capacity; compact chiller

---

### 1. Introduction

Due to the increasing energy consumption of air-conditioning in building and the need to reduce CO<sub>2</sub> emissions to the environment, the interest of using renewable energy sources shows up stronger than ever. Solar energy, often correlated to the cooling demand of a building [1], is probably one of the best energy resources for air conditioning systems. The major part of the solar cooling systems use thermally driven single effect absorption chiller [2], which are available on the market in a wide range of capacities and designed for different applications. But only few chillers are available with a cooling capacity lower than

---

\* Corresponding author. Tel.: +33-479-444-588; fax: +33-479-621-374.  
E-mail address: [francois.boudehenn@cea.fr](mailto:francois.boudehenn@cea.fr).

50 kW and with an optimized design for solar applications [3]. For small scale applications, like single family house, there are only few available chillers (less than 10 kW). Therefore the development of low power cooling and air conditioning systems is of particular interest [4]. There are two main working pairs for absorption chillers: water-lithium bromide and ammonia-water. Ammonia-water chillers are particularly interesting because of their low production and maintenance cost [5]. Moreover the high pressure thermodynamic cycle is favorable for internal heat and mass transfer optimization, reduction of the ammonia-water solution quantity, lower hydraulic pressure drops and a compact final design. The 5 kW cooling capacity ammonia-water absorption chiller described in this paper was especially designed for solar cooling applications in this way.

### Nomenclature

|            |                                    |        |
|------------|------------------------------------|--------|
| $COP_{th}$ | Thermal coefficient of performance | [-]    |
| P          | Thermal Power                      | [W]    |
| $\Delta P$ | Pressure drop                      | [Pa]   |
| T          | Temperature                        | [°C]   |
| M          | Mass flow rate                     | [kg/h] |

### Subscripts

|     |                       |
|-----|-----------------------|
| E   | Evaporator            |
| AC  | Absorber-Condenser    |
| G   | Generator or Desorber |
| RS  | Rich Solution         |
| In  | Inlet                 |
| Out | Outlet                |

## 2. Numerical studies

A model of a single-stage ammonia-water cycle (Fig. 1) was implemented in EES [6]. The mass and energy conservation equations have been carried out for each component [7] with correlations of Ibrahim and Klein [8] to calculate thermodynamic properties of the  $NH_3/H_2O$  mixture. Solution and refrigerant are assumed to be at saturation at exit of each component (no limitation of heat and mass transfer). By specifying operating temperatures conditions, solution mass flow or cooling load required, heat exchangers efficiencies of solution heat exchanger and subcooler (Fig. 1.) and pressure drop in each components, the software provides corresponding thermodynamic states of the cycle and the global performances. This model was used to design the prototype and to perform parametric studies.

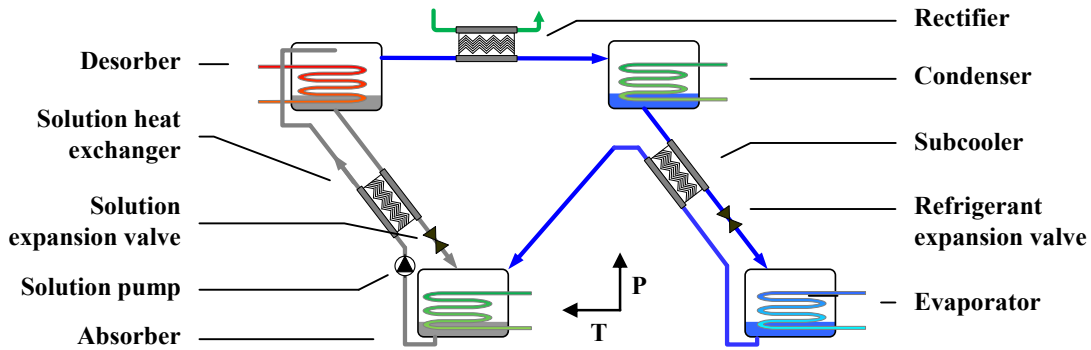


Fig. 1. Scheme of the thermodynamic cycle used

Simulations showed the interest to have a pump with variable-speed to adapt the cooling power when the operating conditions change (Fig. 2.).

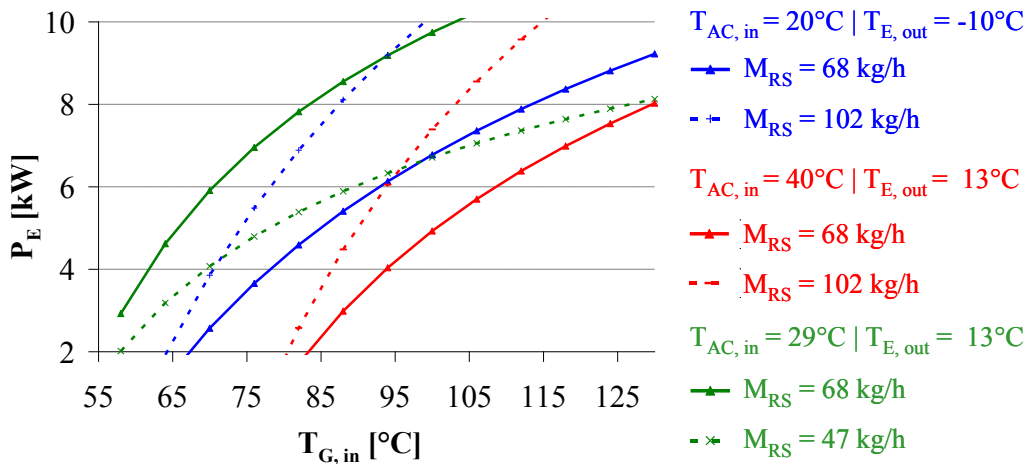
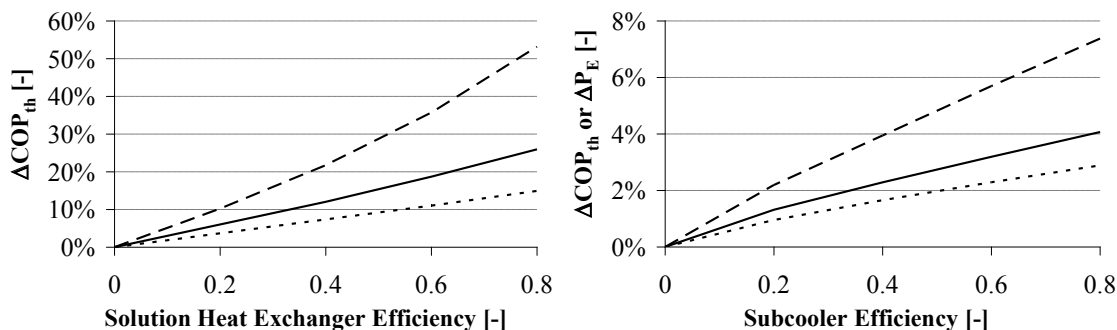


Fig. 2. Solution flow impact on cold power for different operating temperature conditions

Thanks to internal heat exchangers efficiency studies, we pointed out that the solution heat exchanger efficiency improves significantly the thermal COP whereas the subcooler efficiency has a small effect (Fig. 3. a and b). Furthermore, the solution heat exchanger allows to sub-cool the poor solution before the expansion valve, so that no desorption occurs when the solution is throttled before entering the absorber.



—  $T_{E, out}/T_{AC, in}/T_{G, in} = 15/30/75^{\circ}C$  ···  $T_{E, out}/T_{AC, in}/T_{G, in} = 15/25/130^{\circ}C$  ···  $T_{E, out}/T_{AC, in}/T_{G, in} = -10/25/100^{\circ}C$

Fig. 3. (a)  $COP_{th}$  improvement as a function of the solution heat exchanger efficiency for different temperature conditions; (b)  $COP_{th}$  improvement as a function of the subcooler efficiency for different temperature conditions

The internal pressure drops in the components impact more the cooling power production than the thermal coefficient of performance: at nominal inlet conditions ( $T_E/T_{AC}/T_G = 18/27/80^{\circ}C$ ), if pressure drop in each component is equal to 5 kPa, then the thermal COP degradation is only 1% while the cooling capacity degradation is 5%. It reveals also that the absorber and the subcooler are the only components sensitive to pressure drop in terms of thermodynamic cycle’s performance (Table 1).

Table 1.  $\Delta P$  component impact on COP degradation (hyp: each component has the same  $\Delta P$ )

|  | Absorber | Condenser | Desorber | Evaporator | Subcooler | Solution Heat Exchanger | Rectifier |
|--|----------|-----------|----------|------------|-----------|-------------------------|-----------|
| $\Delta P$ component impact on thermal COP degradation | 47,0%    | 3,1%      | 4,7%     | -0,3%      | 42,2%     | -0,4%                   | 2,1%      |

### 3. Technical choices and design

Since ammonia is very corrosive against many common materials, a special care was taken by selecting only ammonia compliant components. As a technological readiness asset, only industrial brazed/soldered plate heat exchangers are implemented, which means that some modifications have to be done to turn three of them (desorber, rectifier and absorber, Fig. 1.) into mass transfer components. Three stainless steel tanks are used as vapor-liquid separator at the outlets of those exchangers. The rectifier heat exchanger removes remaining water from ammonia vapor before the condenser. The absorber heat exchanger’s inlet features an original double distributor system, which allows liquid and gas phases to be evenly fed into each channel.

Table 2. Design values (rated min max) for components and solution pump (external fluid)

|                     |         | Evaporator | Condenser | Absorber | Desorber | Pump     |
|---------------------|---------|------------|-----------|----------|----------|----------|
| Temperature<br>[°C] | Nominal | 18         | 27        | 27       | 75       | 32       |
|                     | Minimal | -10        | 15        | 15       | 60       | 32       |
|                     | Maximal | 18         | 45        | 45       | 130      | 50       |
| Pressure<br>[bar]   | Nominal | 6.2        | 12.4      | 6.2      | 12.4     | 6.2/12.4 |
|                     | Minimal | 2          | 8.7       | 2        | 8.7      |          |
|                     | Maximal | 6.2        | 20        | 6.2      | 20       | 6.2/20   |
| Power [kW]          | Nominal | 5          | 5         | 7.5      | 8        | 0.55     |

Since the solution pump is the major electricity consuming component of the chiller and therefore directly related to the electrical coefficient of performance, special attention was paid to its specifications with regard to hydraulic, environmental, user and electrical constraints. High guarantee of tightness is required because of the high ammonia toxicity for human beings as well as an accurate speed control over wide operating range as stated in Table 2. It leads to the selection of a diaphragm pump as solution pump. Since the liquid solution entering into the pump comes from the absorber, its temperature is relatively close to saturation. If some frictional heating occurs, there is a risk of desorption around the moving parts, which can severely alter lifespan. Therefore, the selected pump must show very little heating, even locally on its inner parts.

The usual control components for ammonia systems are available for large capacities. Thermostatic expansion valves for instance could not be found for the capacity of this project. Although some machines do use a time regulated valve, this requires a substantial fluid volume for achieving a smooth thermodynamic cycle. Since the current machine shows a very low fluid volume, electronically regulated valves were selected.

Table 3. Sensors number and measurement characteristics

| Sensors type                               | Number | Uncertainty (+/-)  |
|--|--------|--------------------|
| Heat transfer fluid temperature (Pt)       | 10     | 0.1K               |
| Refrigerant temperature (TC)               | 15     | 0.3K               |
| Refrigerant pressure (0-10bar and 0-40bar) | 6      | 0.2% full scale    |
| Refrigerant flowrate (Coriolis)            | 2      | 0.2%               |
| Liquid level (Capacitive)                  | 4      | 0.5%               |
| Density (Coriolis)                         | 2      | 2kg/m <sup>3</sup> |

Since the pump and electronic valves are powered through electronic power controllers, the input current to the devices differs significantly in shape and amplitude from the maximum rated supply current and looks highly non-linear. Therefore we checked the signal before starting the measurement campaigns with an oscilloscope and we compared it with the measured values from electronic power meter transducer used for online recording. Those maximum ratings were 230 Vac – 5 A with an accuracy of 0.5% full scale.

Control and monitoring are based on a 1s time step and the actuators (3 internal valves and pump, 3 external pumps) are controlled to ensure a safe and automatic operation of the chiller.

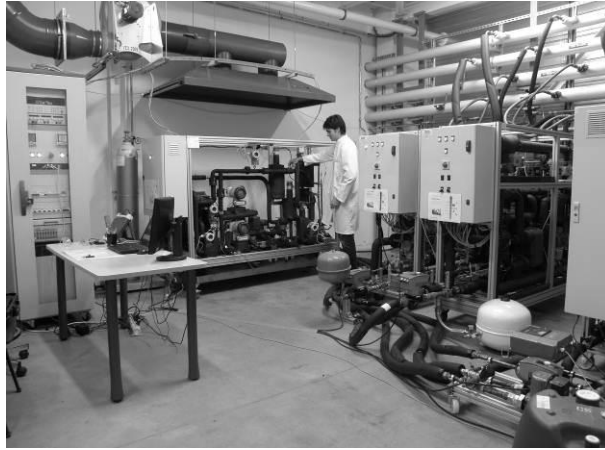


Fig. 4. Picture of the 5 kW ammonia-water chiller prototype connected to the INES experimental test bench

#### 4. Experimental and numerical results comparison

Experimental tests were performed at INES (French National Institute for Solar Energy) facilities (Fig. 4.) providing adjustable power and temperature level for cooling or heating on the ports of the chiller.

Due to the technical choices, the quantities of water and ammonia contained in the prototype are very low, with 0.735 kg of water and 2.4 kg of ammonia. The specific solution and refrigerant charge is close to 0.6 kg per kW.

The first results have shown a 4.2 kW cooling capacity at 80, 27 and 18°C at the inlets of desorber, absorber/condenser and evaporator respectively. The experimental thermal COP, defined as the ratio between cooling and heating energy, is about 0.65 in these conditions while a poor efficiency (0.16 instead of 0.83 planned) of the solution heat exchanger was detected.

Experimental thermal COP values are compared to the numerical ones as a function of the Carnot efficiency [3] (Fig. 5.). In Fig. 5, besides the experimental and numerical results, the second curve (Market correlation) represents a global view of the performances of five commercial single-stage absorption chillers that were characterized at INES facilities. This graphic enables the comparison of absorption chillers regardless of their cooling capacity. The experimental results are far from the numerical ones; it is partly explained by the poor efficiency of the solution heat exchanger as shown in Fig. 3 (a). Furthermore, it was observed during the tests that a good tuning of the solution throttle valve, hence of the poor solution loop pressure drop, improves the performances of the chiller. Consequently, the latest results seem to fit the numerical curve better. Undergoing work on the control strategy is aimed at reducing the gap.

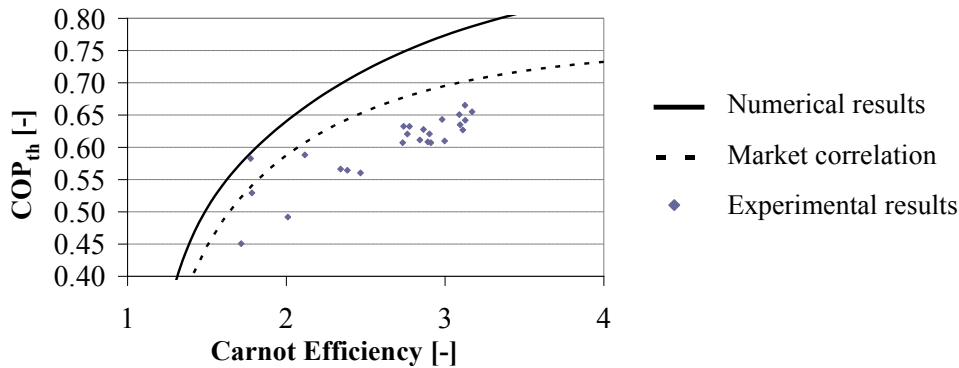


Fig. 5. Comparison of the numerical and experimental thermal COP as a function of the Carnot efficiency

A first characterization of the absorption chiller with a constant inlet temperature of 18°C at the evaporator was carried out for different temperatures at the Absorber/Condenser inlets, from 25°C to 35°C.

In Fig. 6, the impact of the rich solution flow on the evaporator power was studied and in Fig. 7, it was the generator inlet temperature, from 70°C to 90°C. The dotted curves represent the results of the numerical model where the parameters were chosen to correspond to experimental operating conditions:

- internal temperatures at the outlet of the evaporator, condenser, rectifier and desorber,
- rich solution mass flow rate,
- solution heat exchanger and the subcooler efficiencies,
- pressure drop in the absorber.

Since the temperature at the evaporator inlet is not an input of the numerical model, the vapour quality of the refrigerant at the evaporator outlet was fitted to obtain the same evaporation temperature as during the tests. Furthermore, the vapour temperature entering the rectifier is supposed equal to the temperature of the desorber outlet minus 5°C. This hypothesis, going against the assumption of Herold & al. [7], is made to obtain a vapour temperature close to the ones measured.

Fig 6 and 7 as Fig.5 show a significant gap between experimental and numerical data, though the slopes of the curves are close. This gap can be explained by the poor performances of the absorber, where the mass transfer rate is limited. The cooling power decrease when the temperature at the absorber and condenser inlets is increased, as shown by both experimental and numerical results. However, the cooling power is relatively constant at  $T_{AC, in} = 35^{\circ}\text{C}$  (Fig. 6) and we didn't achieve a test at low flow rate at these temperature because the prototype behaviour wasn't stable enough under these operating conditions. The near asymptotic behaviour of the experimental curve at  $T_{AC, in} = 25^{\circ}\text{C}$  (Fig. 6) and at  $T_{G, in} = 90^{\circ}\text{C}$  curve for low absorber/condenser temperature (Fig. 7) indicate performances limitation of the chiller.

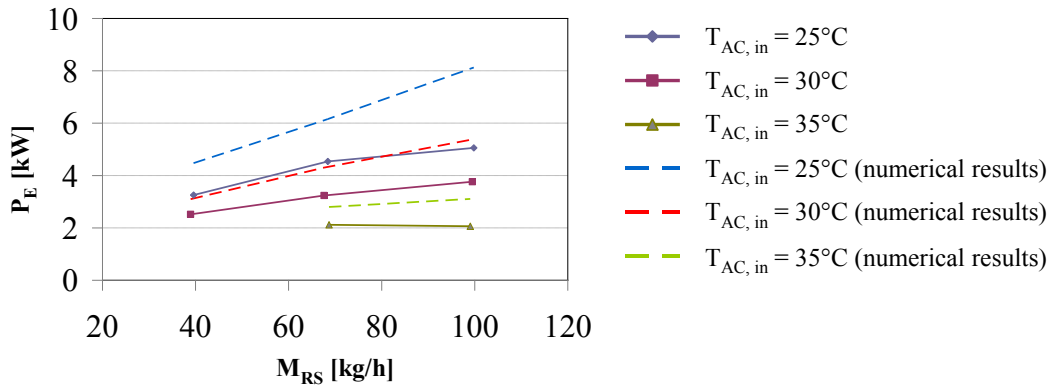


Fig. 6. Thermal power at the evaporator vs. rich solution mass flow rate for different absorber/condenser inlet temperatures

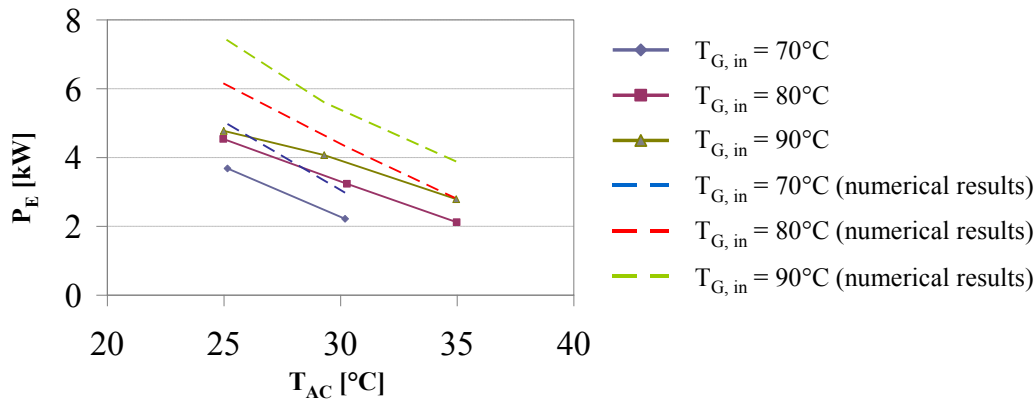


Fig. 7. Thermal power at the evaporator vs. inlet temperature of the Absorber/Condenser hydraulic loop for different generator inlet temperatures

## 5. Conclusions

This article presents the development of a 5 kW cooling capacity ammonia-water absorption chiller for solar cooling applications. The objective of small overall dimensions, low cost and low ammonia load leads us to choose compact flat plate heat exchangers available from the market.

The different technical choices enable to build a compact chiller with low solution and refrigerant quantities, even in the case of a prototype.

The first experimental results are very encouraging. Nevertheless, further optimization points have been identified, especially for the solution heat exchanger and the absorber. These components will be replaced soon by adapted in order to enhance the performance.

The last experimental tests with adapted control strategy showed results close to numerically expected ones. The next step is to develop an optimized control strategy that is maximizing performance of the chiller in various real operating conditions.



## Acknowledgements

Part of this work was financed by the French Carnot Institute “Energie du Futur”, in the framework of the SOLAMMOR project.

## References

- [1] Lecuona A, Ventas R, Venegas M, Zacarias A, Salgado R. Optimum hot water temperature for absorption solar cooling. *Solar Energy* 83, 1806-1814, 2009.
- [2] Grossman G. Solar-powered system for cooling, dehumidification and air-conditioning. *Solar Energy* 72 (1), 53-62, 2002.
- [3] Henning HM. Solar assisted air conditioning of buildings – an overview. *Applied Thermal Engineering* 27, 1734-1749, 2007.
- [4] Balaras CA, Grossman G, Henning HM, Infante Ferreira CA, Podesser E, Wang L, Wiemken E. Solar air conditioning in Europe – an overview. *Renewable and Sustainable Energy reviews* 11, 299-314, 2007.
- [5] Wang RZ, Ge TS, Chen CJ, Ma Q, Xiong ZQ. Solar sorption cooling systems for residential applications : options and guidelines. *International Journal of Refrigeration* 32, 638-660, 2009.
- [6] EES : Engineering Equation Solver, <http://www.fchart.com/>.
- [7] Herold, K. E., Radermacher, R. et Klein, S. A. *Absorption Chillers and Heat Pumps*. CRC Press, 1996.
- [8] Ibrahim, O.M., Klein, S.A. Thermodynamic Properties of Ammonia-Water Mixtures. *ASHRAE Trans.: Symposia*, 21, 2, 1495-1502, 1993.